

## Electronic structure and optical properties of coupled quantum dots

J. H. Oh and K. J. Chang

*Department of Physics, Korea Advanced Institute of Science and Technology, Taejon 305-338, Korea*

G. Ihm

*Department of Physics, Chungnam National University, Taejon 305-764, Korea*

S. J. Lee

*Department of Physics, Korea Military Academy, Seoul 139-799, Korea*

(Received 21 November 1995)

We calculate the electronic structure of quantum dots coupled along the growth direction with one or two electrons in magnetic fields. We examine the spin transitions of the ground states and the optical transitions between the energy levels, which are associated with far-infrared absorption. Because of the dot-dot and electron-electron interactions, the coupled quantum dots exhibit rich electronic structures. We suggest that the effects of these interactions on the energy spectra are observable by optical measurements because the transition energies exhibit discontinuous changes for a vertically polarized light as the magnetic field increases.

Recent advances in nanostructure semiconductor technology make it possible to tailor quasi-zero-dimensional electron systems, i.e., quantum dots, at semiconductor interfaces by patterning isolated metallic gates or etching vertically quantum wells.<sup>1,2</sup> Since the size of a quantum dot is comparable to the effective Bohr radius of a host semiconductor, the quantum dot gives rise to discrete energy levels and is referred to as an artificial atom where the number of electrons and confinement potential are controlled artificially. Usually, one considers two-dimensional or disklike quantum dots with the lateral size much larger than the extent in the growth direction. Then, the electronic energy levels of the disklike quantum dot are mainly determined by the lateral motion. Most theoretical and experimental studies have been so far focused on the electronic structure and the transport behavior of a single disklike quantum dot.<sup>1-5</sup>

A coupled quantum dot that could be considered as an artificial molecule has attracted much attention recently.<sup>6-9</sup> In contrast to the single disklike quantum dot, one must consider another degree of freedom along the growth direction for a vertically coupled quantum dot, while the circular symmetry is lost for a laterally coupled quantum dot. The main feature in this system is the effects of dot-dot and electron-electron interactions on the electronic structure. Several theoretical and experimental studies were done to investigate the effects of electron-electron and dot-dot interactions on the electron tunneling in coupled quantum dots.<sup>7-9</sup> Discrete resonance peaks in the current-voltage curves were observed, and each resonance peak was attributed to the quantum tunneling between the electronic energy levels. However, since tunneling experiments are strongly influenced by contacts, it is very difficult to extract only the effect of electron-electron interaction.

In this work we study the electronic structure of a vertically coupled quantum dot in magnetic fields and calculate the oscillator strength for optical transitions to see the effects of dot-dot and electron-electron interactions. A structural parameter such as the barrier width is varied over a wide range

of magnetic field in calculating the energy levels. From the exact diagonalization of the Hamiltonian matrix, we find that the dot-dot and electron-electron interactions strongly affect the ground state of the coupled quantum dots, which can be measured by optical experiments. For the light polarized along the growth direction, several resonance frequencies are found, exhibiting blueshift and sharp drops with the increase of magnetic field, while independently of the magnetic field this behavior cannot be seen in the absence of the Coulomb interaction. We also present the phase diagram for the singlet and triplet transitions of the ground state as a function of magnetic field and barrier width.

A coupled quantum dot is characterized by a parabolic potential with the confinement frequency  $\omega_0$  on the  $xy$  plane, which is well accepted as a model of the realistic confining potential.<sup>10,11</sup> Along the growth direction, we use the vertical potential  $V(z)$ , which consists of two square wells with the equal width of  $w_w=150$  Å, a barrier with a width of  $w_b=50$  Å, and two buffer layers with a thickness of 350 Å. We choose the barrier height of 147 meV to represent the  $\text{Al}_{0.2}\text{Ga}_{0.8}\text{As}/\text{GaAs}$  system, and the effective mass  $m^*=0.0665m_0$ .

For an external magnetic field  $\vec{B}=B\hat{z}$ , the Hamiltonian for the coupled quantum dot with a single electron is written in cylindrical coordinates,

$$H^0 = \frac{1}{2m^*} (\vec{p} + e\vec{A})^2 + \frac{1}{2} m^* \omega_0^2 \rho^2 + V(z), \quad (1)$$

where  $\vec{A} = \vec{B} \times \vec{\rho} / 2$  is the vector potential. Since the vertical and lateral motions of a single electron are decoupled, the eigenvalues and eigenfunctions of the single particle Schrödinger equation  $H^0 \psi^0(\rho, \varphi, z) = E^0 \psi^0(\rho, \varphi, z)$  are easily calculated,

$$E_{N,L,k}^0 = E_{N,L}^R + \varepsilon_k^z = \hbar \omega \left( N + \frac{|L|}{2} + \frac{1}{2} \right) + \frac{L}{2} \hbar \omega_c + \varepsilon_k^z, \quad (2)$$

$$\psi^0(\rho, \varphi, z) = \chi_{N,L}(\rho, \varphi) \phi_k(z),$$

$$\chi_{N,L}(\rho, \varphi) = \frac{1}{\sqrt{2\pi\lambda}} \sqrt{\frac{N!}{(N+|L|)!}} e^{iL\varphi} e^{-\xi/2} \xi^{|L|/2} L_N^{|L|}(\xi), \quad (3)$$

where  $\phi_k(z)$  and  $\chi_{N,L}$  denote the solutions for the vertical and lateral motions, respectively,  $\xi = \rho^2/\lambda$ ,  $\lambda = \hbar/m^*\omega$ , and  $L_N^L$  is a Laguerre polynomial. Here, the frequency  $\omega = \sqrt{\omega_c^2 + 4\omega_0^2}$  indicates a measure of hybrid effects between the magnetic and electric confinements with the cyclotron frequency  $\omega_c = eB/m^*$ . It is noted that the energy levels  $E_{N,L}^R$  for the lateral motion depend on both the radial ( $N=0, 1, 2, \dots$ ) and azimuthal ( $L = 0, \pm 1, \pm 2, \dots$ ) quantum numbers because our system is symmetric about the  $z$  axis. The effect of the dot-dot interaction appears only in the energy levels ( $\varepsilon_k^z$ ) associated with the  $z$  motion. As the separation between two square-well potentials decreases, the dot-dot interaction  $v$  induces two states, i.e., the bonding ( $\varepsilon_a^z = \varepsilon^0 - v$ ) and antibonding ( $\varepsilon_b^z = \varepsilon^0 + v$ ) states, where  $\varepsilon^0$  is the energy of an isolated single quantum dot. For dipole transitions that are associated with far-infrared absorption, two resonance frequencies,  $\omega_+ = (\omega + \omega_c)/2$  and  $\omega_- = (\omega - \omega_c)/2$ , exist for a laterally polarized light due to parabolic lateral confinement.<sup>3,11</sup> For the  $z$ -polarized light, the dipole transitions are allowed between the bonding and antibonding states, i.e., between the  $\varepsilon_a^z$  and  $\varepsilon_b^z$  states; however, the transition energy is independent of magnetic field.

If two electrons are confined in a coupled quantum dot, the Hamiltonian is given by

$$H = H^0(1) + H^0(2) + \frac{e^2}{4\pi\epsilon_0\epsilon|\vec{r}_1 - \vec{r}_2|} + \frac{g^*\mu_B}{\hbar} \vec{B} \cdot \vec{S}, \quad (4)$$

where  $H^0(i)$  is the Hamiltonian of a single particle in Eq. (1),  $\epsilon$  is the dielectric constant of GaAs,  $g^*$  is the effective  $g$  factor,  $\mu_B$  is the Bohr magneton, and  $\vec{S}$  is the spin angular momentum. To solve this many-body Hamiltonian, we transform the coordinates  $\{\vec{\rho}_1, \vec{\rho}_2, z_1, z_2\}$  into  $\{\vec{\eta} = (\vec{\rho}_1 + \vec{\rho}_2)/2, \vec{\rho} = (\vec{\rho}_1 - \vec{\rho}_2), z_1, z_2\}$ . Then, the Hamiltonian of Eq. (4) becomes

$$H = H_R(\vec{\eta}) + H_r(\vec{\rho}, z_1, z_2) + \frac{g^*\mu_B}{\hbar} \vec{B} \cdot \vec{S}. \quad (5)$$

Here  $H_R$  represents the lateral component of the center-of-mass motion,

$$H_R = (\vec{P} + e\vec{A}_R)^2/2M + M\omega_0^2\eta^2/2, \quad (6)$$

where  $\vec{P}$  is the lateral component of  $\vec{p}_1 + \vec{p}_2$  with  $M = 2m^*$  and  $\vec{A}_R = \vec{B} \times \vec{\eta}$ . The energy levels and eigenfunctions of  $H_R$  have the same forms as  $E_{N,L}^R$  and  $\chi_{N,L}$ , except for  $\lambda = \hbar/M\omega$ . The Hamiltonian  $H_r$  is written

$$H_r = \frac{1}{2\mu} (\vec{p}_r + e\vec{A}_r)^2 + \frac{1}{2}\mu\omega_0^2\rho^2 - \frac{\hbar^2}{2m^*} \left( \frac{\partial^2}{\partial z_1^2} + \frac{\partial^2}{\partial z_2^2} \right) + V(z_1) + V(z_2) + \frac{e^2}{4\pi\epsilon_0\epsilon\sqrt{\rho^2 + (z_1 - z_2)^2}}, \quad (7)$$

where  $\vec{p}_r$  is the lateral component of  $(\vec{p}_1 - \vec{p}_2)/2$ ,  $\mu = m^*/2$ , and  $\vec{A}_r = \vec{B} \times \vec{\rho}/4$ . Since our system is rotationally symmetric about the  $z$  axis, the angular momentum is a good quantum number. Writing the wave function of  $H_r$  as  $\psi_{n,l} = e^{il\varphi} R(\rho, z_1, z_2)/\sqrt{2\pi}$ , the equation for  $R(\rho, z_1, z_2)$  becomes

$$\left[ -\frac{\hbar^2}{2m^*} \left( \frac{1}{\rho} \frac{\partial}{\partial \rho} \rho \frac{\partial}{\partial \rho} - \frac{l^2}{\rho^2} \right) + \frac{\hbar\omega_c}{2} l + \frac{m^*}{16} \omega^2 \rho^2 - \frac{\hbar^2}{2m^*} \left( \frac{\partial^2}{\partial z_1^2} + \frac{\partial^2}{\partial z_2^2} \right) + V(z_1) + V(z_2) + \frac{e^2}{4\pi\epsilon_0\epsilon\sqrt{\rho^2 + (z_1 - z_2)^2}} \right] R_{nl} = E_{nl}^r R_{nl} \quad (8)$$

with the eigenvalues  $E_{nl}^r$  and the azimuthal angular momentum  $\hbar l$ . Then, we expand  $R_{nl}$  in terms of  $\chi_{n,l}$  and  $\phi_i$  in Eq. (3), which are the eigenfunctions for the lateral and vertical motions, respectively, for the single-particle case,

$$R_{n,l}(\rho, z_1, z_2) = \sum_{m,i,j} C_{mij}^{nl} \chi_{m,l}(\rho/2\lambda^2, 0) \phi_i(z_1) \phi_j(z_2) \quad (9)$$

with  $\lambda = \hbar/\mu\omega$ .

The energy levels  $E_{n,l}^r$  are calculated for both the single and coupled quantum dots. For a single quantum dot with  $w_w = 150 \text{ \AA}$  and  $\hbar\omega_0 = 4 \text{ meV}$ , the electronic structure is very similar to that of the disklike quantum dot.<sup>3,4</sup> In this case, since the energy difference between the first and second lowest states for the  $z$  motion is larger than that for the radial motion  $\hbar\omega$ , the lowest-energy states mainly result from the hybridization of the radial motions, with the wave function approximated as  $R_{n,l}(\rho, z_1, z_2) \approx \phi_1(z_1) \phi_1(z_2) \sum_m C_m^{nl} \chi_{m,l}(\rho/2\lambda^2, 0)$ . Since  $R(\rho, z_1, z_2)$  is invariant under particle permutation, the symmetry is determined by the angular momentum; i.e., the wave functions with even (odd) quantum numbers  $l$  have a singlet (triplet) spin state.

For a coupled quantum dot, the energy difference between the two lowest states for the  $z$  motion is comparable to that for the radial motion. The symmetry of the wave function for  $H_r$  depends on both the  $z$  and lateral motions. If electron-electron interactions are excluded, one can describe the lowest-energy level  $E_{nl}^r$  for a given orbital angular momentum by  $|l, b, b\rangle$ ; i.e., two electrons occupy the bonding state for the  $z$  motion. In this case, the second lowest levels denoted as  $|l, a, b\rangle$  and  $|l, b, a\rangle$  are degenerate, while in the third level  $|l, a, a\rangle$  two electrons occupy the antibonding states. When electron-electron interactions turn on, the energy levels are shifted to higher energies due to the repulsive Coulomb interaction and the degenerated second levels split into the symmetric and antisymmetric states for particle permutation, approximately,  $|l, m\rangle = |l, 1\rangle \approx (|l, a, b\rangle + |l, b, a\rangle)/2$  and  $|l, 2\rangle \approx (|l, a, b\rangle - |l, b, a\rangle)/2$ . Here each occupation of two electrons is represented by the quantum number  $m$ ;  $|l, m\rangle = |l, 0\rangle \approx |l, b, b\rangle$  and  $|l, 3\rangle \approx |l, a, a\rangle$ . Because of the Pauli exclusion principle, the  $|l, 2\rangle \approx (|l, a, b\rangle - |l, b, a\rangle)/2$

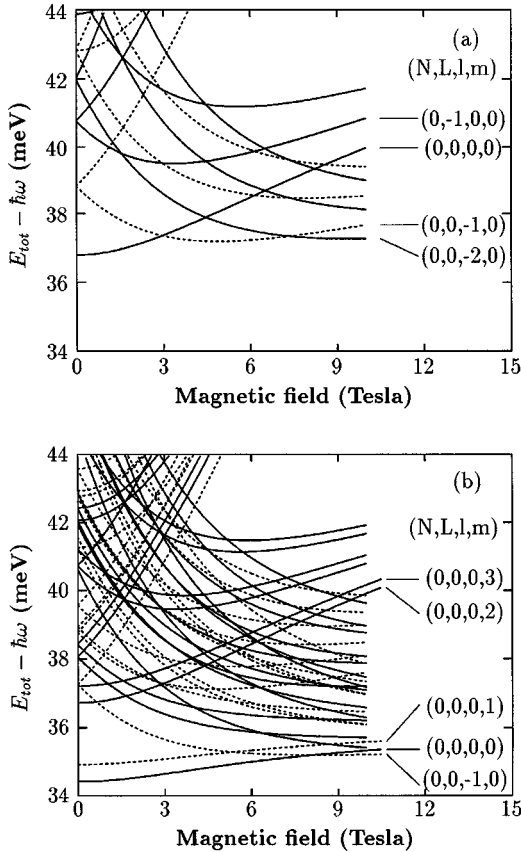


FIG. 1. The total energies of two electrons are drawn as a function of magnetic field for the (a) single and (b) coupled quantum dots with  $\hbar\omega_0 = 4$  meV. The spin singlet and triplet states are described by solid and dotted lines, respectively, for  $g^* = 0$ . The quantum numbers  $(N, L, l, m)$  represent the  $|N, L\rangle|l, m\rangle$  states.

state is regarded as a spin triplet state for even angular momentums  $\hbar l$ , while it is a spin singlet state for odd angular momentums.

The magnetic-field dependences of the total energies  $E_{\text{tot}} = E_{N,L}^R + E_{l,m}^r$  are plotted for the single and coupled quantum dots in Fig. 1. For the single quantum dot, the ground state exhibits the orbital angular momentum change as the magnetic field increases, similar to the disklike quantum dot.<sup>3,4,12</sup> These ground-state transitions are understood in terms of the Coulomb and kinetic energies. As the magnetic field increases, both the kinetic and Coulomb energies for low angular momentum states increase more rapidly than for higher angular momentum states. Thus, the angular momentums of the ground state follow the sequence of  $l=0, -1, -2, \dots$  with the increase of the magnetic field. However, the magnetic field  $B_c$  at which the ground-state transition occurs is larger than that found in the disklike quantum dot because the finite size of the vertical motion reduces the Coulomb energy.<sup>12</sup> For the coupled quantum dot, the ground-state transitions exhibit somewhat different behavior [see Fig. 1(b)]. For barrier widths  $w_b < 55$  Å, the transition of the ground state occurs in the same way as the single quantum dot. However, for large barrier widths ( $w_b \geq 60$  Å), a different mechanism for the ground-state transition is found, where the radial, vertical, and spin wave

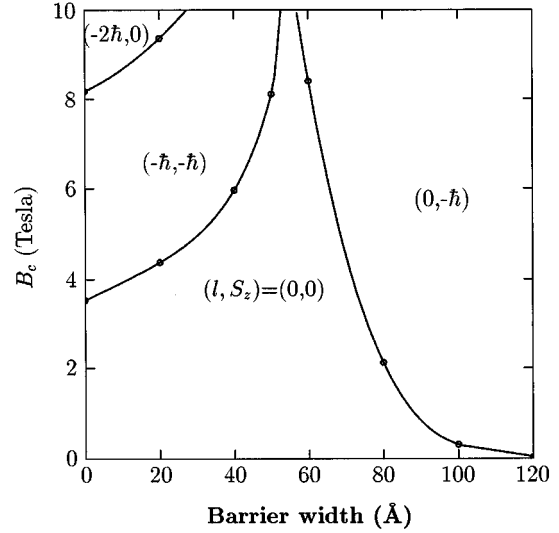


FIG. 2. The phase boundaries of the ground state for the coupled quantum dot are drawn as a function of barrier width for  $w_w = 150$  Å and  $g^* = 0.44$ .

functions of the ground state change abruptly while the orbital angular momentum remains the same, i.e., the transition occurs from  $|l, m\rangle = |0, 0\rangle$  to  $|l, m\rangle = |0, 1\rangle$ . Since the energy of the second lowest state  $|l, m\rangle = |0, 1\rangle$  with  $S_z = -\hbar$  de-

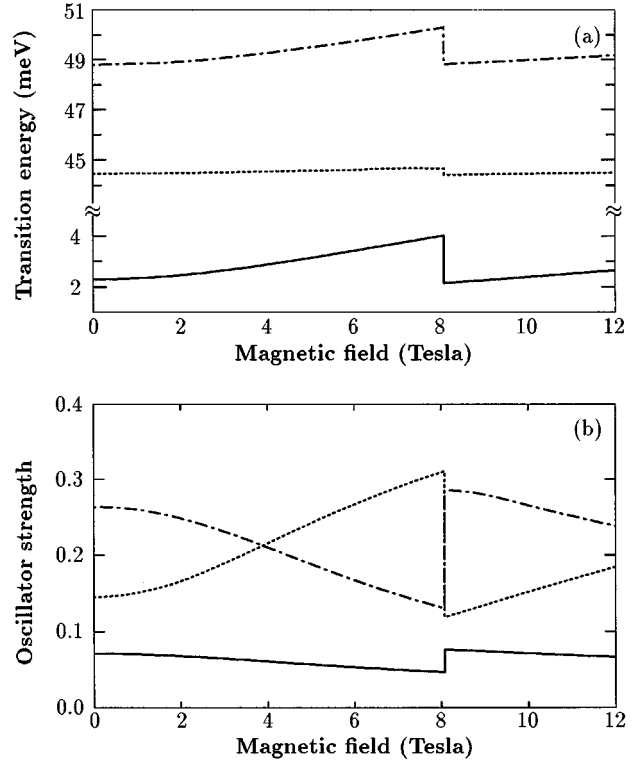


FIG. 3. The transition energies and associated oscillator strengths for the coupled quantum dot are plotted as a function of magnetic field. The transition from  $|N, L\rangle|l, m\rangle = |0, 0\rangle|l, 0\rangle$  to  $|0, 0\rangle|l, 2\rangle$  is denoted by the solid line. See the text for the dotted and dot-dashed lines.

increases by  $g^* \mu_B B$  as the magnetic field increases, this state becomes the ground state at high magnetic fields. This result indicates that as the barrier width increases, two electrons are less correlated and easily spin polarized; i.e.,  $S_z = -\hbar$ , even for low magnetic fields. In this case, the transition field  $B_c$  is strongly influenced by the value of  $g^*$  and the energy difference between the first and second states, which reflect the dot-dot and electron-electron interactions. If the barrier width increases to reduce the dot-dot interaction, the energy difference between the first and second lowest states for  $g^* = 0$  becomes smaller, resulting in a smaller value of  $B_c$ . For  $g^* = 0.44$ , the ground-state transition fields are plotted as a function of barrier width in Fig. 2.

The optical response in the coupled quantum dot with two electrons is different from that of the one-electron case for the vertical polarization because of the electron-electron interaction. From the generalized Kohn theorem,<sup>13</sup> dipole absorptions by a laterally polarized light can only probe the center-of-mass motion in a strictly parabolic potential, thus it is inadequate for seeing any effect due to electron-electron interactions. However, for the vertically polarized light, it may be possible to observe the effect of electron-electron interactions on the electronic structure. In Fig. 3, we show the calculated oscillator strength and the transition frequencies excited from the ground state of the coupled quantum dot with  $w_b = 50 \text{ \AA}$ . As the magnetic field increases, the resonance energies are blueshifted and show discontinuous drops at about 8 T, while independently of the magnetic field this behavior is not found in the absence of the Coulomb interaction. The discontinuous drops are originated from the spin transition of the ground state at which the ground state is

abruptly changed from  $|l, m\rangle = |0, 0\rangle \approx |0, b, b\rangle$  to  $|-1, 0\rangle \approx |-1, b, b\rangle$  state. Three resonance energies in Fig. 3 strongly depend on the dot-dot and electron-electron interactions, and are attributed to the transitions from  $|l, b_1, b_1\rangle$  to  $(|l, a_1, b_1\rangle + |l, b_1, a_1\rangle)/2$ ,  $(|l, a_1, b_2\rangle + |l, b_2, a_1\rangle)/2$ , and  $(|l, a_2, b_1\rangle + |l, b_1, a_2\rangle)/2$ , which are represented by the solid, dotted, and dot-dashed lines, respectively. Here,  $a_i$  ( $b_i$ ) represents the bonding (antibonding) state splitted from the  $i$ th sublevel of the  $z$  motion in the single quantum dot. For large barrier widths ( $w_b \geq 60 \text{ \AA}$ ), we also find discontinuous changes of the resonance energies and the associated oscillator strengths as the magnetic field increases. Thus, we suggest that the transition of the ground states and the dot-dot and electron-electron interactions can be observed with the vertically polarized light. However, this feature is not sensitive to the choice of the lateral confining potential because it is mainly originated from the square-well potential along the vertical direction.

In conclusion, we have investigated the electronic structure and the optical properties of the vertically coupled quantum dot in magnetic fields. Because of the dot-dot and electron-electron interactions as well as the hybrid effect between the magnetic and electric confinements, the coupled quantum dot exhibits rich electronic structures. We find that the effects of the electron-electron and dot-dot interactions on the energy levels can be detectable with far-infrared light polarized along the growth direction.

This work was supported in part by the Korea Research Foundation, by the Ministry of Education, by the SPRC of Jeonbuk National University, and by the CMS of Korea Advanced Institute of Science and Technology.

<sup>1</sup>R. C. Ashoori, H. L. Stormer, J. S. Weiner, L. N. Pfeiffer, K. W. Baldwin, and K. W. West, *Phys. Rev. Lett.* **71**, 613 (1993); M. A. Reed, *Sci. Am.* **268**, 98 (1993).

<sup>2</sup>M. Van Hove, R. Pereira, W. De Raedt, G. Borghs, R. Jonckheer, C. Sala, W. Magnus, W. Schoenmaker, and M. Van Rassum, *J. Appl. Phys.* **72**, 158 (1992).

<sup>3</sup>U. Merkt, J. Huser, and M. Wagner, *Phys. Rev. B* **43**, 7320 (1991).

<sup>4</sup>P. A. Maksym and T. Chakraborty, *Phys. Rev. Lett.* **65**, 108 (1990); D. Pfannkuche, V. Gudmundsson, and P. A. Maksym, *Phys. Rev. B* **47**, 224 (1991).

<sup>5</sup>L. P. Kouwenhoven, F. W. J. Hekking, B. J. Van Wees, C. J. P. M. Harmans, C. E. Timmering, and C. T. Foxon, *Phys. Rev. Lett.* **65**, 361 (1990); P. L. McEuen, E. B. Foxman, U. Meirav, M. A. Kastner, Y. Meir, N. S. Wingreen, and S. J. Wind, *ibid.* **66**, 1926 (1991).

<sup>6</sup>C. Y. Fong, H. Zhong, and B. M. Klein, *Phys. Rev. B* **49**, 7466 (1994); T. Chakraborty, V. Halonen, and P. Pietilainen, *ibid.* **43**,

14 289 (1991).

<sup>7</sup>M. Tewordt, H. Asahi, V. J. Law, R. T. Syme, M. J. Kelly, D. A. Ritchie, A. Churchill, J. E. F. Frost, R. H. Hughes, and G. A. C. Jones, *Appl. Phys. Lett.* **60**, 595 (1992); M. Tewordt, R. J. F. Hughes, L. Martin-Moreno, J. T. Nicholls, H. Asahi, M. J. Kelly, V. J. Law, D. A. Ritchie, J. E. F. Frost, G. A. C. Jones, and M. Pepper, *Phys. Rev. B* **49**, 8071 (1994).

<sup>8</sup>G. Bryant, *Phys. Rev. B* **48**, 8024 (1993); G. Klimeck, G. Chen, and S. Datta, *ibid.* **50**, 2316 (1994).

<sup>9</sup>J. J. Palacios and P. Hawrylak, *Phys. Rev. B* **51**, 1769 (1995).

<sup>10</sup>C. Sikorski and U. Merkt, *Phys. Rev. Lett.* **62**, 2164 (1989).

<sup>11</sup>C. T. Liu, K. Nakamura, D. C. Tsui, K. Ismail, D. A. Antoniadis, and H. I. Smith, *Appl. Phys. Lett.* **55**, 168 (1989).

<sup>12</sup>J. H. Oh, K. J. Chang, G. Ihm, and S. J. Lee, *Phys. Rev. B* **50**, 15 397 (1994).

<sup>13</sup>L. Brey, N. F. Johnson, and B. I. Halperin, *Phys. Rev. B* **40**, 10 647 (1989).